



Published in final edited form as:

*Invest New Drugs*. 2013 October ; 31(5): 1142–1150. doi:10.1007/s10637-013-9932-0.

## Polycationic calixarene PTX013, a potent cytotoxic agent against tumors and drug resistant cancer

**Ruud P. M. Dings,**

Department of Biochemistry, Molecular Biology & Biophysics, University of Minnesota, Minneapolis, MN 55455, USA

**Joseph I. Levine,**

Department of Biochemistry, Molecular Biology & Biophysics, University of Minnesota, Minneapolis, MN 55455, USA

Department of Chemistry, University of Minnesota, Minneapolis, MN 55455, USA

**Susan G. Brown,**

Department of Chemistry, University of Minnesota, Minneapolis, MN 55455, USA

**Lucile Astorgues-Xerri,**

INSERM U728 and Department of Medical Oncology, Beaujon University Hospital, (AP-HP – PRES Paris 7 Diderot), 100 bd du Général Leclerc, 92110 Paris-Clichy, France

**John R. MacDonald,**

PepTx, Inc., Excelsior, MN, USA

**Thomas R. Hoye,**

Department of Chemistry, University of Minnesota, Minneapolis, MN 55455, USA

**Eric Raymond, and**

INSERM U728 and Department of Medical Oncology, Beaujon University Hospital, (AP-HP – PRES Paris 7 Diderot), 100 bd du Général Leclerc, 92110 Paris-Clichy, France

**Kevin H. Mayo**

Department of Biochemistry, Molecular Biology & Biophysics, University of Minnesota, Minneapolis, MN 55455, USA

Kevin H. Mayo: mayox001@umn.edu

---

©Springer Science+Business Media New York 2013

Correspondence to: Kevin H. Mayo, mayox001@umn.edu.

RPM Dings and JI Levine contributed equally to this work.

**Electronic supplementary material** The online version of this article (doi:10.1007/s10637-013-9932-0) contains supplementary material, which is available to authorized users.

**Conflict of interest** Co-authors K.H. Mayo and J. R. MacDonald have a financial interest in PepTx, a pharmaceutical company that holds license to commercialize the PTX compounds

### Author contribution

Participated in research design

Ruud P.M. Dings, John R. MacDonald, Thomas R. Hoye, Eric Raymond, and Kevin H. Mayo.

Conducted experiments

Ruud P.M. Dings, Joseph I. Levine, Susan G. Brown, Lucile Astorgues-Xerri.

Performed data analysis and wrote the paper

All authors.

## Summary

Previously, we reported on the anti-tumor activities of two designed calix[4]arene-based topomimetics (PTX008 and PTX009) of the amphipathic, angiostatic peptide Anginex. Here, we chemically modified the hydrophobic and hydrophilic faces of PTX008 and PTX009, and discovered new calixarene compounds that are more potent, cytotoxic anti-tumor agents. One of them, PTX013, is particularly effective at inhibiting the growth of several human cancer cell lines, as well as drug resistant cancer cells. Mechanistically, PTX013 induces cell cycle arrest in sub-G1 and G0/G1 phases of e.g. SQ20B cells, a radio-resistant human head and neck carcinoma model. In the syngeneic B16F10 melanoma tumor mouse model, PTX013 (0.5 mg/Kg) inhibits tumor growth by about 50-fold better than parent PTX008. A preliminary pharmacodynamics study strongly suggests that PTX013 exhibits good in vivo exposure and a relatively long half-life. Overall, this research contributes to the discovery of novel therapeutics as potentially useful agents against cancer in the clinic.

## Keywords

Calixarenes; Galectin-1; Structure-activity relationships; Therapeutics

---

## Introduction

FDA approval of new anti-cancer agents has decreased over the past decade, and many of those approved therapeutics are usually antibodies or compounds that target molecular entities within the same pathway(s) of previously approved agents, e.g. growth factors and related kinase inhibitors. In general, this mind-set has hindered the development of new classes of compounds for treating cancer [1]. Moreover, targeting the same component(s) within the same pathway (s) has contributed to limited therapeutic effectiveness, partly due to cancer cell selection of alternative pathways and developed drug resistance. Clearly, there is a need for alternative approaches and paradigms to drug discovery and development.

There are two general strategies to therapeutic drug discovery: target-based and activity-based. Target-based drug discovery involves first identifying compounds that bind specifically to a therapeutically validated molecular target. Recent developments in genomics (e.g. the human genome project) and the emergence of increasing proteomics insights have encouraged and promoted the target-based approach [1, 2]. The activity- or phenotypic-based approach dominated drug discovery prior to the molecular age, and was largely based on testing a diverse set of compounds (e.g. natural products, substrate analogues, combinatorial syntheses) using in vitro cell-based assays followed by in vivo assessment of toxicity and efficacy [1–3]. Ideally, identification of the drug target and mechanism of action would follow during later stages of the drug development process [2].

Although in recent years the activity-based approach had become less favored in the pharmaceutical industry, it is undergoing a renaissance because of shortcomings with the molecular-based approach that cannot, e.g., predict issues related to in vivo toxicity and in vivo efficacy. It is at this level that most drugs fail in development. Because of this, the current paradigm to drug discovery more often employs a combination of these approaches.

Initial identification of an effective compound in cell-based and initial animal studies results in efforts to identify the molecular target and to elucidate structure– activity relationships (SAR) that contribute to further lead optimization [2].

Previously, we used the activity-based approach to discover that the amphipathic  $\beta$ -sheet peptide 33mer Anginex is an angiostatic and anti-tumor agent [4–8] and then identified galectin-1 (gal-1) as its molecular target [5–8]. Subsequently, we designed topomimetics of Anginex using the calix[4]arene scaffold, which is particularly well-suited for face-selective functionalization in order to impart facial amphiphilicity [9, 10], and identified two compounds (PTX008 and PTX009, Fig. 1) as potent anti-tumor agents [11]. Recently, we reported that PTX008, like Anginex, also targets gal-1, and it does so at a site different from the gal-1 canonical carbohydrate binding site [12]. In this regard, PTX008 functions as a non-competitive, allosteric inhibitor of galectin-1 function. PTX008 is currently in a human Phase I clinical trial.

Here, we report on four new calixarene compounds (Fig. 1) that we have also observed to have cytotoxic and anti-tumor properties. Of these, PTX013, at sub-micromolar concentrations, was most effective at inhibiting cancer cell proliferation, in particular that of drug resistant tumor cells. In the syngeneic B16F10 melanoma mouse model, PTX013 inhibited tumor growth by up to 80 % at a dose of 0.5 mg/Kg. Overall, this research contributes to our ability to design therapeutic agents that inhibit tumor growth, potentially useful in the clinic.

## Experimental

### Chemicals and chemistry

Calix[4]arene PTX008 (PepTx, Excelsior MN; USA) is also known as OTX-008 (OncoEthix, Lausanne; Switzerland) and was synthesized as previously described, wherein it was referred to as 0118 [11]. PTX009 was synthesized as previously described, wherein it was referred to as calixarene compound 1097 [11]. The four new calixarene compounds (PTX012–PTX015) discussed here were synthesized using similar approaches. The details of these syntheses as well as the spectroscopic characterization of all new compounds are provided as Supplemental Material.

### Cell lines

Human umbilical vein derived EC (HUVEC), fibroblasts and MA148, a human epithelial ovarian carcinoma cell line were kindly provided by Prof. Dr. S. Ramakrishnan (University of Minnesota) and cultured as described earlier [5, 7, 8, 11, 13]. HUVEC and fibroblasts were cultured in gelatin-coated tissue-culture flasks (0.2 %) in culture medium [RPMI 1640 with 20 % (v/v) human serum, supplemented with 2 mM glutamine, 100 units/mL penicillin and 0.1 mg/mL streptomycin]. Murine cell lines: endothelial (2H11), melanoma (B16F10), mammary carcinoma (SCK), and fibrosarcoma (FSaII) were kindly provided by Prof. Dr. R. Griffin [5, 13, 14] and human cell lines: lung carcinoma (A549), head and neck carcinoma (SQ20B), breast adenocarcinoma (MCF- 7), and colon adenocarcinoma (Colo205 and DLD-1) were obtained from ATCC (Rockville, MD, USA) or National Cancer Institute collection (Bethesda, MD, USA). The resistant SQ20B-R cell line was developed from the

head and neck SQ20B cancer cell line by inducing acquired resistance to PTX008. The resistant MCF7-R cell line was developed by knocking down WISP-2/CCN5 by RNA interference in estrogen receptor alpha positive MCF-7 breast cancer cells [15]. The resistant Colo205-R cell line was developed from the colon Colo205 cancer cell line by inducing acquired resistance to ingenol-3-angelate (a protein kinase C modulator); this line additionally displayed cross-resistance to Enzastaurin (Eli Lilly) [12, 16]. The resistant DLD-R cell line was developed from the colon DLD-1 cell line by inducing conditional expression of the human transcriptional repressor Snail [17]. Both murine and human cell lines were cultured on non-coated flasks using 10 % fetal bovine serum and 1 % penicillin/streptomycin in RPMI 1640 as described before [5, 13, 18] and regularly checked to confirm absence of *Mycoplasma*.

### Cytotoxicity assay

All cell types were seeded at a concentration of 3,000 cells per well and allowed to adhere for at least 3 h at 37 °C in 5 % CO<sub>2</sub>/95 % air before treatments were initiated. The cells were then exposed to various concentrations of calixarenes for 72 h. Colorimetric assays [CCK-8 (Dojindo; Gaithersburg, MD) and MTT (Sigma; Saint-Quentin Fallavier, France)] were used to assess cell viability relative to untreated cells, as described earlier [6, 12, 19, 20]. All measurements were done in triplicate, and the experiments were done at least three times.

### Cell cycle analysis

Cell cycle analysis was assessed by flow cytometry. In brief, cells were seeded onto 25 cm<sup>3</sup> flasks and treated with various concentrations of PTX013. At various time-points adherent and non-adherent cells were recovered, washed with PBS, fixed in 70 % ethanol and stored at 4 °C until use. Cells were rehydrated in PBS, incubated for 20 min at room temperature with 250 µg/mL RNAse A, and for 20 min at 4 °C with 50 µg/mL propidium iodide in the dark. The cell cycle distribution and percentage of apoptotic cells were determined with a flow cytometer [FACSCalibur and Cell Quest Pro software (BD, Le-Pont-de-Claix, France)].

### Tumor mouse model

Female C57/BL6 mice were purchased from the Jackson Laboratories and allowed to acclimate to local conditions for at least 1 week. Animals were given water and standard chow ad libitum and were kept on a 12-h light/dark cycle. Experiments were approved by the University of Minnesota Research Animal Resources ethical committee. Exponentially growing B16/F10 cells were cultured, harvested, suspended in serum free RPMI (2.0×10<sup>6</sup> cells/mL), and 100 µL was inoculated subcutaneously (s.c.) into the right flank of the mice (*n*=10 each group), as described previously [5, 8, 19]. Studies were carried out in a therapeutic intervention model with established tumors to test the capacity of treatment to inhibit tumor growth [6]. Tumors were allowed to grow to the size of approximately 75 mm<sup>3</sup> prior to randomization and initiation of treatment. Compounds were administered via intraperitoneal (IP) injection twice daily (BID) in the concentrations indicated. Tumor volume was determined by measuring the size of the tumors on the flanks of the mice. The diameters of tumors were measured using callipers (Scienceware; Pequannock, NJ), and the

volume was calculated using the equation to determine the volume of a spheroid:  $(a^2 \times b \times \pi) / 6$ , where  $a$  is the width of the tumor and  $b$  is the length of the tumor. As an indirect measurement of general toxicity, body weights of mice were monitored twice weekly using a digital balance (Ohaus; Florham, NJ).

## Results and discussion

### Synthesis of calixarenes

Given the relatively good therapeutic potential of calixarenes PTX008 and PTX009 [11], we performed this focused SAR study by modifying the hydrophobic and hydrophilic faces of these compounds as shown in Fig. 1. To test the effect of having a different molecular footprint to the calixarene scaffold, we synthesized calix[6]arene PTX012 that maintains the chemical character of both hydrophobic and hydrophilic faces of PTX008, but with a larger footprint due to addition of two aromatic moieties within the calixarene scaffold. PTX013 has the same footprint and hydrophobic face as PTX008, but has shorter 2-dimethylaminoethoxy groups on its hydrophilic face vis-à-vis the larger and somewhat more polar *N*-(2-dimethylamino)ethyl acetamido groups. PTX014 and PTX015 were designed as hybrids. PTX014 has the hydrophobic face of PTX009 and the hydrophilic face of PTX008, whereas PTX015 has the hydrophobic face of PTX008 and the hydrophilic face of PTX013. We then assessed the functional efficacy of these compounds for their ability to inhibit the proliferation of cancer cells, including drug resistant cells, and the growth of tumors in murine models.

### Cytotoxicity studies

We first assessed the ability of these calixarenes (Fig. 1) to induce cytotoxicity in eight different cell types: two normal, primary cells [human umbilical vein endothelial cells (HUVEC) and fibroblasts]; immortalized mouse endothelial cells (2H11), and five cancer cell lines (the human MA148 ovarian carcinoma and A549 lung adenocarcinoma and the murine SCH breast carcinoma, FSaII fibrosarcoma, and B16F10 melanoma). Dose response curves are shown in Fig. 2 as the percentage of cell survival relative to that from cultures treated only with vehicle (100 %). Data points represent the means obtained in at least three independent experiments, each using triplicate cell cultures. Apparent  $IC_{50}$  values (i.e., the concentration required for 50 % cell viability) derived from these curves are given in Table 1 and compared with those from PTX008 and PTX009.

PTX013 and PTX015 were the most effective at inducing cytotoxicity in a variety of cell types tested. For example, PTX013 and PTX015 had an  $IC_{50}$  of 2  $\mu$ M against HUVEC. Whereas PTX015 revealed a similar single digit micromolar activity ( $\sim$ 2  $\mu$ M) against most cell types, PTX013 generally achieved  $IC_{50}$  values ranging from 0.2  $\mu$ M to 2  $\mu$ M. Overall, PTX013 demonstrated the greatest cytotoxic effects. Results from PTX013 and PTX015 showed markedly increased potency over the cytotoxicity profiles of PTX008 and PTX009, which on average exhibited mid-single-digit micromolar  $IC_{50}$  values (Table 1).

The absence of significant activity from PTX012 allows us to conclude that enlarging the calixarene molecular footprint greatly attenuates activity. This is interesting, because we

recently reported that PTX008 targets galectin-1 as a non-competitive, allosteric inhibitor [12]; therefore, increasing the calixarene footprint suggests that there would be weaker interactions between the calixarene scaffold and the lectin. Moreover, increased activity with PTX013 and PTX015 vis-à-vis PTX014 indicates that reducing the length of the hydrophilic, tertiary amine substituents and/or decreasing their polarity by removing the amide linkage group significantly improves function. These data also suggest that PTX013 and PTX015 probably do not target galectin-1, because the cell proliferation inhibitory profile of PTX008 against these cell types is quite different from those of PTX013 and PTX015 (see Fig. 2 and Table 1).

Because PTX013 was overall the most active compound, we performed further cell cytotoxicity studies with it using four drug resistant, human cancer cell lines (Colo205-R, SQ20B-R, MCF7-R, and DLD-R) that all demonstrate an epithelial to mesenchymal transition (EMT) phenotype. The Colo205-R cell line was derived from Colo205 cells with an acquired resistance to protein kinase C modulators like Enzastaurin (LY317615-HCl, Eli Lilly) [16, 21]. SQ20B-R cells were derived from inherent radio-resistant SQ20B head & neck squamous cancer cells with acquired resistance to PTX008 that developed after about 6 months of treatment. MCF7-R is derived from the breast cancer cell line MCF-7 by knocking down WISP-2/CCN5 [15]. The DLD-R cell line was generated from the human DLD-1 epithelial colon cell line by inducing conditional expression of the human transcriptional repressor Snail [17].

PTX013 exhibited a strong cytotoxic effect with  $IC_{50}$  values of about 3  $\mu$ M or less against all four parental cell types (Fig. 3a). More importantly, PTX013 shows the same activity against their drug resistant, EMT analogs. In general, PTX013 functions more like a cytotoxic drug than a cytostatic agent, like PTX008 and various kinase inhibitors. As exemplified with SQ20B cells in Fig. 3b, exposure to PTX013 induces sub-G1 DNA fragmentation that can be either due to cell necrosis or to apoptosis. Furthermore, cell cycle analysis reveals that exposure of these cells to PTX013 induces accumulation in G0/G1 phase, suggesting a reduction in DNA synthesis. Besides the differential activity profile of PTX008 and PTX013, since SQ20B and Colo205 cells express relatively low levels of galectin-1, SQ20B-R cells show a loss of gal-1 expression (data not shown), and MCF-7 cells express high levels of galectin-1, these cytotoxicity data further support the proposal that the cellular mechanisms of action of PTX008 and PTX013 are quite different.

### Tumor growth inhibition studies in mice

We assessed the efficacy of the most active of these calixarenes PTX013 and PTX015 (along with PTX008, PTX009 and phosphate buffered saline vehicle) in the B16F10 tumor mouse model. These compounds were administered (IP BID) in a total dose of 10 mg/kg/mouse for 8 days (q1dx8), with treatment being initiated when tumors were approximately 75 mm<sup>3</sup> in size. Compared to PBS controls, PTX013 was observed to be the most effective of these calixarenes at inhibiting B16F10 tumor growth, and even appeared to promote tumor growth regression at this dose (Fig. 4a). In addition, although tumors in all groups generally grew more rapidly post treatment, tumor growth in mice treated with PTX013 occurred more slowly than in all other groups.

As an indirect measure of toxicity, Fig. 4b plots animal body weights during the course of this study. Whereas body weights of mice treated with PTX008 and PTX009 remained constant during the course of treatment, the body weights of mice treated with PTX015, and especially with PTX013, fell significantly. With PTX013, treatment was halted on day 6 because 1 out of 10 of these mice died and the others showed significant reductions (~20 %) in body weights. In all instances, however, animal body weights regained normally post-treatment.

In a subsequent B16F10 tumor growth study, we demonstrated that acute toxicity could be minimized while maintaining efficacy from PTX013 at reduced doses. Figure 5 shows results from a dose response study performed at PTX013 concentrations of 10, 5, 1.5, 0.5, 0.2, and 0.1 mg/kg (q1dx10). PTX013 inhibited tumor growth in a dose dependent manner (Figs. 5a and c). Even though PTX013 was most effective at 10 mg/kg, the compound remained highly effective even down to the dose of 0.2 mg/kg. On day 6 of treatment, tumor growth inhibition was about 50 % and 75 % at 0.2 mg/Kg and 0.5 mg/Kg, respectively, vis-à-vis about 90 % at 1.5 mg/kg or 5 mg/kg.

Trends in body weights shown in Figs. 5b and c indicate that apparent toxicity from PTX013 is considerably less at these lower doses. Still, some acute toxicity was noted at the higher doses (10 mg/kg and 5 mg/kg), where again treatment was halted on day 6 when 1/10 mice died in either group, and the others showed that body weights on average dropped by about 20 %. Local rashes were also observed at the site of injection. In all instances, however, animal body weights increased normally and the rashes resolved post-treatment. At 0.5 mg/kg, body weights were rather constant throughout the entire study, whereas at 0.1 and 0.2 mg/kg, mice gained weight normally during treatment. However, because post-treatment tumor growth occurred at a slower rate in mice treated at the 0.5 mg/kg dose, the optimal IP dose of PTX013 appears to be between 0.2 and 0.5 mg/kg/day, which is 20- to 50-fold lower than that of PTX008 at 10 mg/kg/day.

### Preliminary pharmacodynamics

As an initial read-out on PTX013 pharmacodynamics, we treated mice using different schedules, while maintaining the same cumulative dose of 20 mg/kg throughout the treatment span of 10 days. In this regard, each group of mice ( $n = 10$ ) received either 10 injections of 2 mg/kg/mouse daily (q1dx10), 4 injections of 5 mg/kg/mouse once every 3 days (q3dx4), or 2 injections of 10 mg/kg/mouse once every 5 days (q5dx2). Unexpectedly, the q5dx2 group that received two injections of 10 mg/kg each showed the greatest tumor growth inhibition of about 90 % on day 10 (Fig. 5a), although the second injection was accompanied by a transient body weight loss of about 8 % (Fig. 6b). The lower and more frequently administered doses of 2 mg/kg (10 injections, 1qdx10) and 5 mg/kg (4 injections, q3dx4) suppressed tumor growth to a lesser extent (Fig. 6a) by about 80 % and 70 %, respectively, but without any apparent loss in average body weight (Fig. 5b). Overall, these data strongly suggest that PTX013 has good in vivo exposure and a relatively long half-life.

Calixarene-based compounds PTX008 and PTX009 have been shown previously to be highly effective therapeutic agents against cancer. By chemically modifying the hydrophobic and hydrophilic faces of PTX008 and PTX009, we discovered that two other

calix[4]arenes, PTX013 and PTX015, are highly effective as general cytotoxic agents. The most promising of these, PTX013, is considerably more effective in vitro at inhibiting proliferation of human cancer cells, including various drug resistant cells that have an epithelial to mesenchymal transition (EMT) phenotype. Moreover, PTX013 is highly effective at inhibiting tumor growth in mice. Even at a dose of 0.2 mg/kg, PTX013 inhibits tumor growth with about 20-fold greater potency than PTX008, and preliminary pharmacodynamic data suggest that PTX013 exhibits good in vivo exposure and a relatively long half-life. Future studies are needed to identify the molecular target(s) of PTX013 and PTX015, which appear to be different from the PTX008 target, galectin-1. Overall, this research contributes to the discovery of therapeutics as potentially useful agents against cancer and, especially, against drug resistant cancer in the clinic.

## Supplementary Material

Refer to Web version on PubMed Central for supplementary material.

## Acknowledgments

This work was supported by research grants from the National Institute of Health - National Cancer Institute (CA-096090 and CA-76497) and OncoEthix Inc. to KHM. ER and LA-X were supported by OncoEthix Inc., the Foundation Nelia & Amadeo Barleta (FNAB), and the Association pour la Recherche & l'Enseignement en Cancérologie (AAREC).

## Abbreviations

<b>EC</b>	Endothelial cell
<b>HUVEC</b>	Human umbilical vein EC
<b>SAR</b>	Structural activity relationships
<b>PBS</b>	Phosphate buffered saline

## References

1. Hambley TW, Hait WN. Is anticancer drug development heading in the right direction. *Cancer Res.* 2009; 69(4):1259–1262. [PubMed: 19208831]
2. Dings RP, Mayo KH. A journey in structure-based drug discovery: from designed peptides to protein surface topomimetics as antibiotic and antiangiogenic agents. *Acc Chem Res.* 2007; 40(10): 1057–1065. [PubMed: 17661438]
3. Chen X, Dings RP, Nesmelova I, Debbert S, Haseman JR, Maxwell J, Hoye TR, Mayo KH. Topomimetics of amphipathic beta-sheet and helix-forming bactericidal peptides neutralize lipopolysaccharide endotoxins. *J Med Chem.* 2006; 49(26):7754–7765. [PubMed: 17181157]
4. Griffioen AW, van der Schaft DW, Barendsz-Janson AF, Cox A, Struijker Boudier HA, Hillen HF, Mayo KH. Anginex, a designed peptide that inhibits angiogenesis. *Biochem J.* 2001; 354(2):233–242. [PubMed: 11171099]
5. Dings RP, Loren M, Heun H, McNeil E, Griffioen AW, Mayo KH, Griffin RJ. Scheduling of radiation with angiogenesis inhibitors Anginex and Avastin improves therapeutic outcome to vessel normalization. *Clin Cancer Res.* 2007; 13(11):3395–3402. [PubMed: 17545548]
6. Dings RP, Van Laar ES, Loren M, Webber J, Zhang Y, Waters SJ, Macdonald JR, Mayo KH. Inhibiting tumor growth by targeting tumor vasculature with galectin-1 antagonist anginex



- conjugated to the cytotoxic acylfulvene, 6-hydroxypropylacylfulvene. *Bioconjug Chem.* 2010; 21(1):20–27. [PubMed: 20020769]
7. Dings RP, van der Schaft DW, Hargittai B, Haseman J, Griffioen AW, Mayo KH. Anti-tumor activity of the novel angiogenesis inhibitor anginex. *Cancer Lett.* 2003; 194(1):55–66. [PubMed: 12706859]
  8. Dings RP, Yokoyama Y, Ramakrishnan S, Griffioen AW, Mayo KH. The designed angiostatic peptide anginex synergistically improves chemotherapy and antiangiogenesis therapy with angiostatin. *Cancer Res.* 2003; 63(2):382–385. [PubMed: 12543791]
  9. Ortiz Mellet C, Benito JM, Garcia Fernandez JM. Preorganized, macromolecular, gene-delivery systems. *Chemistry.* 2010; 16(23):6728–6742. [PubMed: 20512821]
  10. Bagnacani V, Franceschi V, Fantuzzi L, Casnati A, Donofrio G, Sansone F, Ungaro R. Lower Rim Guanidinocalix[4]arenes: Macrocyclic Nonviral Vectors for Cell Transfection. *Bioconjug Chem.* 2012; 23:993–1002. [PubMed: 22463059]
  11. Dings RP, Chen X, Hellebrekers DM, van Eijk LI, Zhang Y, Hoye TR, Griffioen AW, Mayo KH. Design of nonpeptidic top-omimetics of antiangiogenic proteins with antitumor activities. *J Natl Cancer Inst.* 2006; 98(13):932–936. [PubMed: 16818857]
  12. Dings RP, Miller MC, Nesmelova I, Astorgues-Xerri L, Kumar N, Serova M, Chen X, Raymond E, Hoye TR, Mayo KH. Antitumor agent calixarene 0118 targets human galectin-1 as an allosteric inhibitor of carbohydrate binding. *J Med Chem.* 2012; 55(11):5121–5129. [PubMed: 22575017]
  13. Dings RP, Williams BW, Song CW, Griffioen AW, Mayo KH, Griffin RJ. Anginex synergizes with radiation therapy to inhibit tumor growth by radiosensitizing endothelial cells. *Int J Cancer.* 2005; 115(2):312–319. [PubMed: 15688384]
  14. Dings RP, Loren ML, Zhang Y, Mikkelsen S, Mayo KH, Corry P, Griffin RJ. Tumour thermotolerance, a physiological phenomenon involving vessel normalisation. *Int J Hyperth.* 2011; 27(1):42–52.
  15. Fritah A, Saucier C, De Wever O, Bracke M, Bieche I, Lidereau R, Gespach C, Drouot S, Redeuilh G, Sabbah M. Role of WISP-2/CCN5 in the maintenance of a differentiated and noninvasive phenotype in human breast cancer cells. *Mol Cell Biol.* 2008; 28(3):1114–1123. [PubMed: 18070926]
  16. Ghoul A, Serova M, Astorgues-Xerri L, Bieche I, Bousquet G, Varna M, Vidaud M, Phillips E, Weill S, Benhadji KA, Lokiec F, Cvitkovic E, Faivre S, Raymond E. Epithelial-to-mesenchymal transition and resistance to ingenol 3-angelate, a novel protein kinase C modulator, in colon cancer cells. *Cancer Res.* 2009; 69(10):4260–4269. [PubMed: 19417139]
  17. De Craene B, Gilbert B, Stove C, Bruyneel E, van Roy F, Berx G. The transcription factor snail induces tumor cell invasion through modulation of the epithelial cell differentiation program. *Cancer Res.* 2005; 65(14):6237–6244. [PubMed: 16024625]
  18. Griffin RJ, Dings RP, Jamshidi-Parsian A, Song CW. Mild temperature hyperthermia and radiation therapy: role of tumour vascular thermotolerance and relevant physiological factors. *Int J Hyperth.* 2010; 26(3):256–263.
  19. Mayo KH, Dings RP, Flader C, Nesmelova I, Hargittai B, van der Schaft DW, van Eijk LI, Walek D, Haseman J, Hoye TR, Griffioen AW. Design of a partial peptide mimetic of anginex with antiangiogenic and anticancer activity. *J Biol Chem.* 2003; 278(46):45746–45752. [PubMed: 12947097]
  20. Dings RP, Van Laar ES, Webber J, Zhang Y, Griffin RJ, Waters SJ, MacDonald JR, Mayo KH. Ovarian tumor growth regression using a combination of vascular targeting agents anginex or topomimetic 0118 and the chemotherapeutic irifolven. *Cancer Lett.* 2008; 265(2):270–280. [PubMed: 18378392]
  21. Serova M, Astorgues-Xerri L, Bieche I, Albert S, Vidaud M, Benhadji KA, Emami S, Vidaud D, Hammel P, Theou-Anton N, Gespach C, Faivre S, Raymond E. Epithelial-to-mesenchymal transition and oncogenic Ras expression in resistance to the protein kinase Cbeta inhibitor enzastaurin in colon cancer cells. *Mol Cancer Ther.* 2010; 9(5):1308–1317. [PubMed: 20406951]

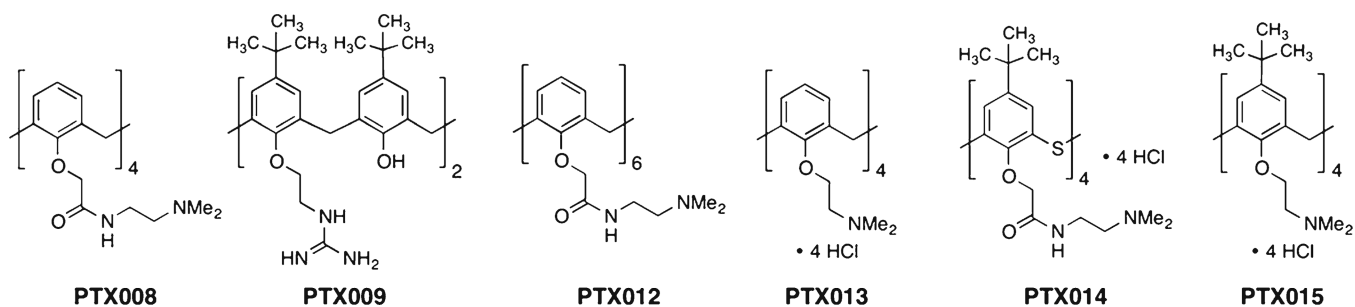


**Fig. 1.** Structural representations of calix[4]arene diguanidine compound PTX009 and tetra-amine compounds PTX008, PTX012, PTX013, PTX014, and PTX015

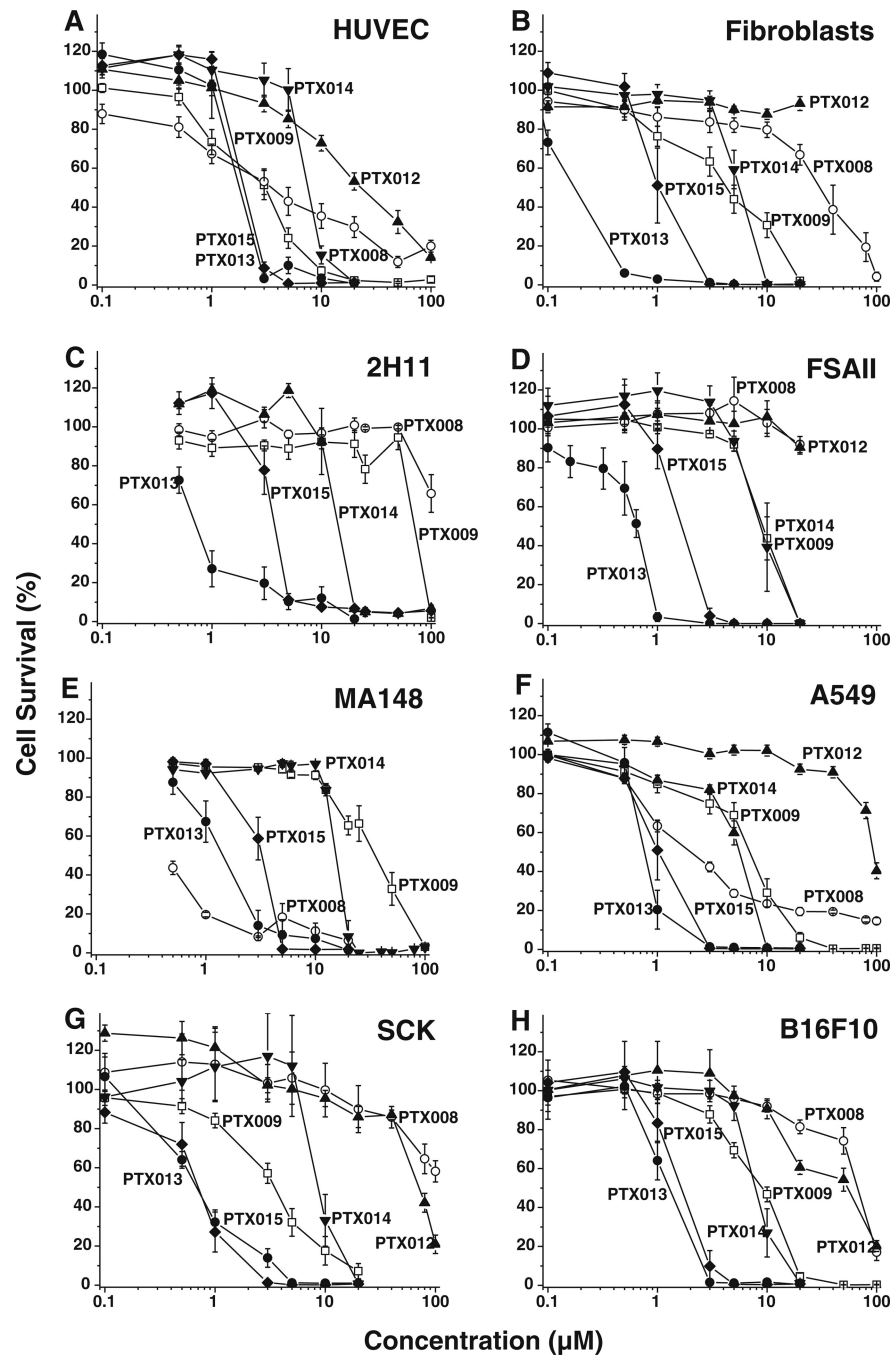


**Fig. 2.** Cytotoxicity effects of calix[4]arenes. Cell viability of HUVEC, fibroblasts, and human ovarian carcinoma (MA148) and lung carcinoma (A549) cells, as well as murine endothelial (2H11), fibrosarcoma (FSaII), mammary carcinoma (SCK), and melanoma (B16F10) cells, was measured in the absence or presence of various concentrations of calixarenes. Cell viability and survival was assessed by colorimetric analysis as described in the “Experimental”

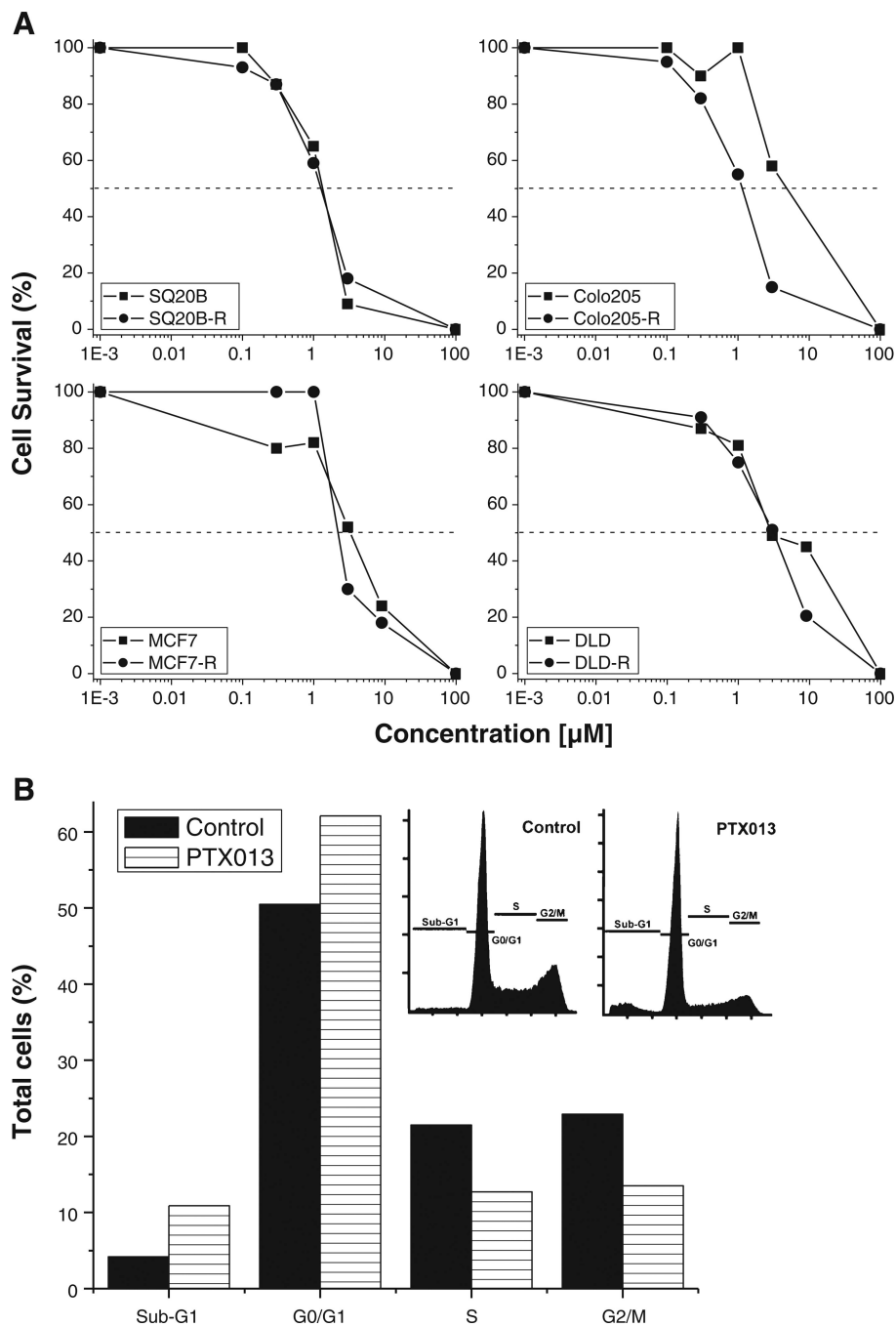


**Fig. 3.** Cytotoxicity effects of PTX013 on human cancer cell lines and corresponding resistant counterparts. **a** Human head and neck carcinoma (SQ20B), colon adenocarcinoma (Colo-205), breast adenocarcinoma (MCF-7), and colon adenocarcinoma (DLD-1) and their respective resistant variations (please see “Material and Methods” for details) were exposed to various concentrations of PTX013 for 72 h. A dose dependent inhibition of cancer cell survival was observed (with an overall approximate  $\text{IC}_{50} \sim 3 \mu\text{M}$ ), as assessed by colorimetric analysis (“Material and Methods”). **b** Cell cycle analysis was performed in

SQ20B cells using PTX013 at 3  $\mu$ M. Exposure to PTX013 increased the number of cells in sub-G1 and G0/G1 phases of the cell cycle and was associated with decreased numbers of cells in S and G2/M phases

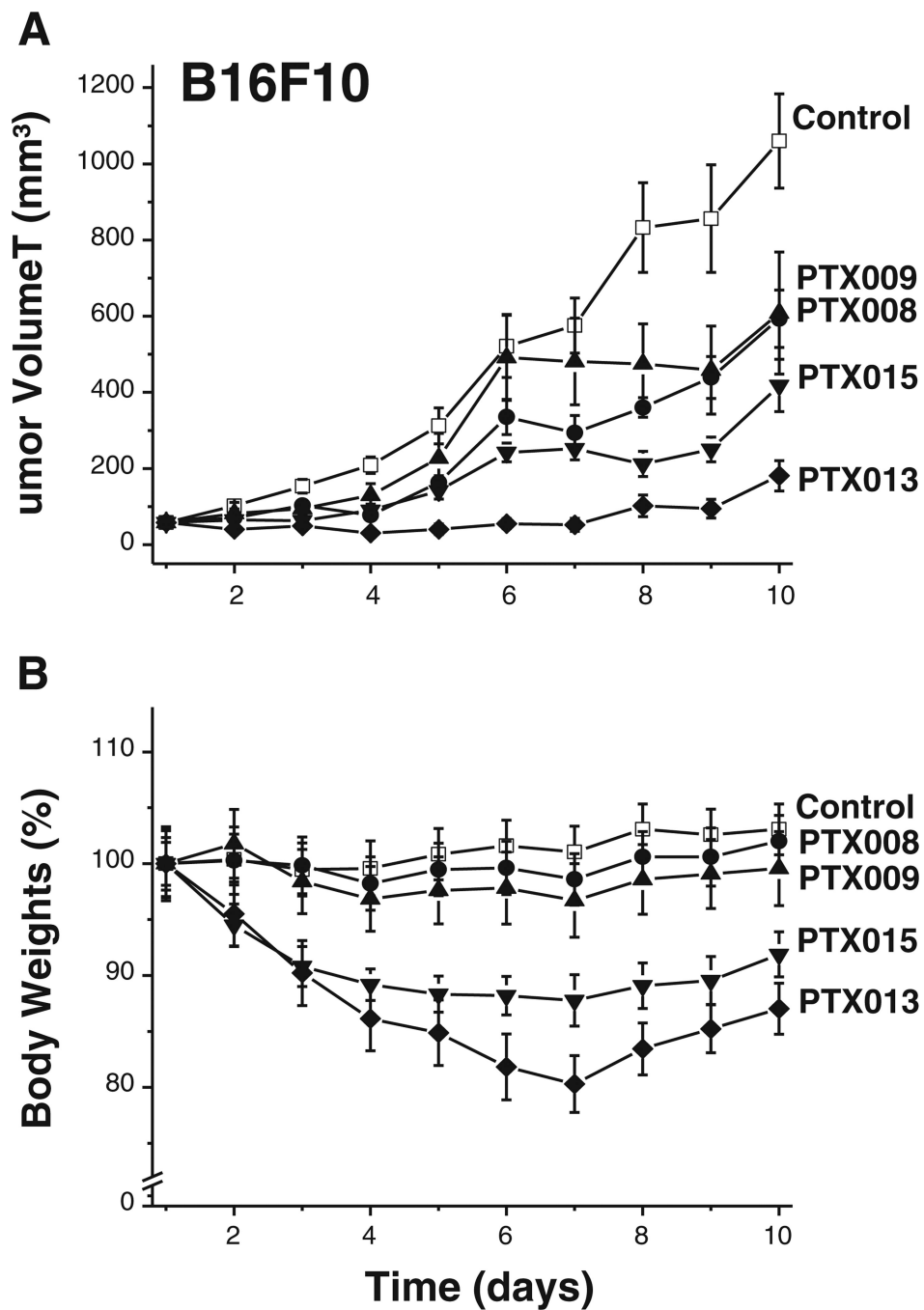


**Fig. 4.** Tumor growth inhibition by calixarenes in the B16F10 melanoma model. **a** B16F10 tumor growth inhibition by calixarenes PTX008, PTX009, PTX013, and PTX015 (10 mg/kg BID IP for 7 days). **b** Body weights of the mice during PTX008, PTX009, PTX013, and PTX015 (10 mg/kg BID IP for 7 days) treatment. Data points represent means $\pm$ SEM ( $n=10$  each group)

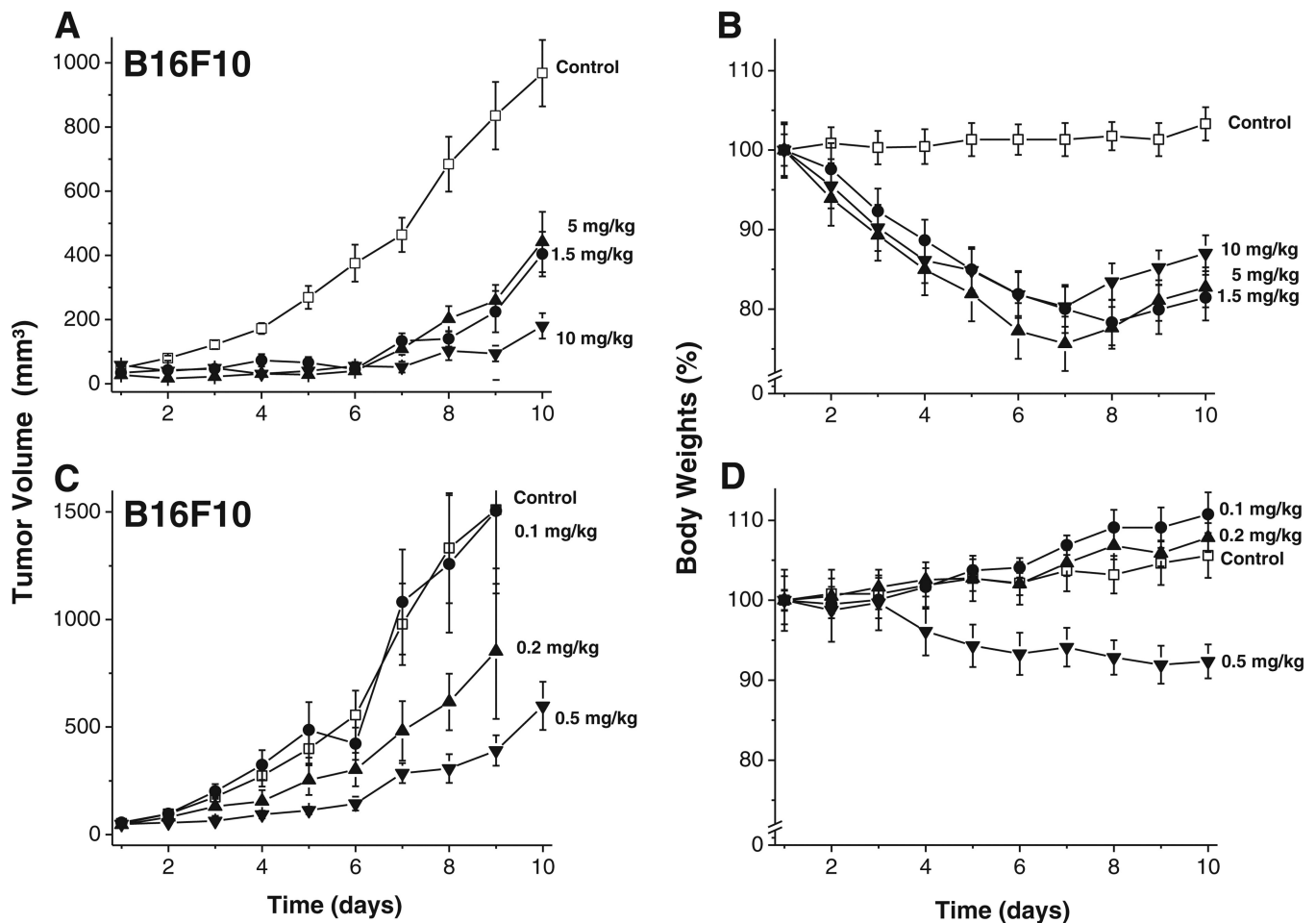


**Fig. 5.** Dose-dependent B16F10 tumor growth inhibition by PTX013 treatment. **a** Dose-dependent B16F10 tumor growth inhibition by 1.5, 5, and 10 mg/kg (BID IP for 7 days) treatment of PTX013. **b** Body weights of the mice during PTX013 treatment (1.5, 5, and 10 mg/kg BID IP for 7 days). **c** Dose-dependent B16F10 tumor growth inhibition by 0.1, 0.2, and 0.5 mg/kg (BID IP for 7 days) PTX013 treatment. **d** Body weights of the mice during PTX013 treatment (0.1, 0.2, and 0.5 mg/kg BID IP for 7 days). Data points represent means $\pm$ SEM ( $n=10-20$  each group)

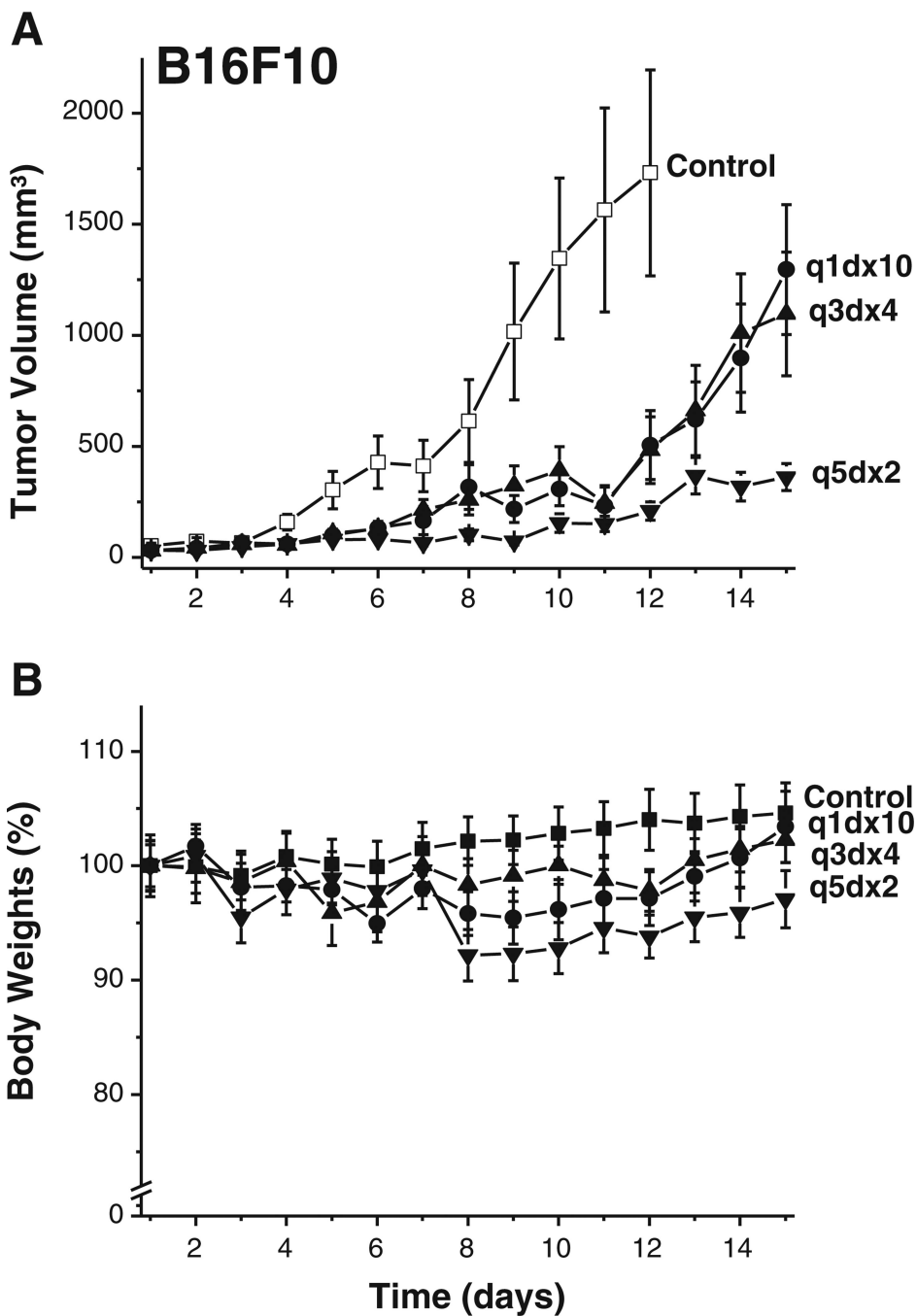


**Fig. 6.** Tumor growth inhibition by PTX013 in the B16F10 melanoma model using different treatment schedules. **a** The effect of different scheduling of PTX013 while maintaining the same accumulative total treatment dose. All groups received a total of 20 mg/kg PTX013 at the end of the treatment span of 10 days. However, the groups were divided to receive either 10 injections of 2 mg/kg every day (q1dx10), 4 injections of 5 mg/kg every 3 days (q3dx4), or 2 injections of 10 mg/kg every 5 days (q5dx2). **b** Body weights of the mice during



different treatment schedules of PTX013. Data points represent means  $\pm$ SEM ( $n=10$  each group)

Table 1

IC<sub>50</sub> values (μM) of calixarene-based compounds on cell viability

	PTX008	PTX009	PTX012	PTX013	PTX014	PTX015
HUVEC	3	3	30	2	8	2
2H11	>100	80	nd	0.7	15	4
Fibroblasts	35	5	>20	0.2	6	1
FSaII	>20	10	>20	0.7	10	2
MA148	0.5	40	nd	1.5	15	3
A549	2	8	100	0.8	6	1
SCK	100	4	100	0.7	9	0.7
B16F10	80	10	70	1	8	2

"nd" indicates not done